R. & M. No. 3719

MINISTRY OF DEFENCE (PROCUREMENT EXECUTIVE)

AERONAUTICAL RESEARCH COUNCIL

REPORTS AND MEMORANDA

An Iterative Method for Calculation of the Loading on a Thin Unswept Wing

By C. C. L. SELLS

Aerodynamics Dept., R.A.E., Farnborough

LONDON: HER MAJESTY'S STATIONERY OFFICE
1973

PRICE £1·35 NET

An Iterative Method for Calculation of the Loading on a Thin Unswept Wing

By C. C. L. SELLS
Aerodynamics Dept., R.A.E., Farnborough

Reports and Memoranda No. 3719*
January, 1972

Summary

A pilot method has been developed, and an EMA computer program written, for the iterative calculation of the load distribution on a thin wing with prescribed warp (downwash). At each iteration the downwash due to the current loading iterate is computed using the author's existing program, and loading corrections are calculated from the downwash difference field until this is sufficiently small. The method has been applied to two rectangular wings of aspect ratio 6, one a flat plate, the other with parabolic camber, and except for a small region near the tip leading edge, has been found to converge quickly, 3 iterations being sufficient to obtain overall accuracy better than 1 per cent in both cases. The method awaits extension to deal with a swept wing.

* Replaces R.A.E. Technical Report 72009—A.R.C. 33 585.

LIST OF CONTENTS

1. Introduction

The author has developed a computer program for the calculation of the induced downwash field on a thin wing with given load distribution[1,2]; here we consider an iterative method, making use of this program, for the inverse problem in which the downwash is prescribed and we have to find the loading.

For this classical problem there already exists a class of collocation methods based on Multhopp's method[3] in which the solution is sought in terms of overall functions (modes), both chordwise and spanwise, whose coefficients are chosen to give the required downwash at certain collocation points. However, in these methods the number of functions available, and hence the overall accuracy, is limited severely by computing considerations, and the methods can be rather sensitive in between the collocation points since, when overall modes are used, a slight perturbation at one point can affect the mode over the whole range and even cause it to oscillate.

In the method to be described below, we set up an iteration cycle in which Prandtl's theory is applied to the downwash field which is given as data, a load distribution is calculated thereby and from that a new downwash field at suitable collocation points according to the method in Refs. 1, 2; then the difference between this downwash field and that given as data is stored and the theory applied to this difference field to produce an extra loading, which is added on to that already existing, and the cycle is repeated until we are satisfied. In Section 2 we give a brief outline of Prandtl's theory up to his celebrated integral equation for the spanwise vorticity (or loading); however, except for the special case of an uncambered wing, Prandtl's theory does not provide an adequate chordwise loading near the wing tip, so in Section 3 we show how we have modified his method (after trial and error) for doing this, and give some preliminary results for the case of a rectangular wing of aspect ratio 6 at unit incidence; in Section 4 we show how these results can be improved, and faster convergence obtained for this problem, by making use of a conjecture of Weber[7] to obtain a better initial approximation for the loading; the conjecture is such that Prandtl's theory can still be used, but his integral equation is somewhat modified. With this refined method, the downwash field converged quickly almost everywhere and after 3 iterations and 2 field calculations, requiring about 15 minutes on an ICL 1907 computer, a third field calculation done as a check showed that it was within 1 per cent of the target field over most of the wing. We say 'almost everywhere' because there is a small region near the tip leading edge where the convergence is severely retarded; the work of Ray and Miller[5,6] shows that for the traditional flat-plate chordwise, elliptic spanwise, loading the downwash becomes logarithmically infinite as this tip is approached, and so unless we employ more suitable loading functions near this tip the method could never converge there, and the difficulty increases the nearer we take our collocation points to it. However, we estimate the loading to be in error by only about 6 per cent of the loading at the centre in this small region, near but not at the tip. Qualitatively similar results were obtained for a wing with the same planform but with parabolic camber.

Since the downwash program[1,2] uses local (panel) modes to represent the loading, and the rest of the program is written to take advantage of this, we hope that our method will not suffer the drawback of the overall modes used by some other collocation methods, that the downwash in between the points where the boundary conditions are actually satisfied may fluctuate unacceptably.

The method is a pilot method only, because it almost certainly needs some modification before it can be applied to a swept wing (with a kink at the centre line). The difficulty here is that unless a very fine mesh is taken near such a centre line, the downwash program[2] is suspect. It is hoped to tackle this problem in due course, perhaps making use of the work of Rossiter.[8]

The program, which of course incorporates the author's downwash program as a subroutine, is written in EMA and occupies less than 12 K words of core store.

2. Preliminaries; Prandtl's Method

We take cartesian coordinates in the wing plane with $0x$ down the centre line (x increasing aft) and $0y$ to starboard. Then if $l(x, y)$ is the wing loading in linear theory, the downwash $\alpha(x, y)$ in the wing plane is given by the principal value (finite part) of the integral:

$$\alpha(x, y) = -\frac{1}{8\pi}\int\int_{\text{wing}} \frac{l(X, Y)}{(Y - y)^2}\left[1 - \frac{X - x}{\{(X - x)^2 + (Y - y)^2\}^{\frac{1}{2}}}\right] dX\, dY. \tag{1}$$

A method for calculating $\alpha(x, y)$ from (1), when $l(x, y)$ is given as data, has been described in Refs. 1, 2. Here we are interested in the inversion problem in which α is prescribed and the distribution of l is sought.

The method to be described is an iterative computer method in which an approximation for l is calculated, and if the downwash field (calculated by the direct method) differs from the datum field, a further approximation is added in an attempt to cancel this difference. At each iteration we shall draw on Prandtl's classical theory[4] to obtain approximations for the spanwise load distribution; it is well to set down some of the details of Prandtl's method, to make our own easier to describe.

For wings of large aspect ratio and zero mean sweep, and in particular unswept at the centre line, by assuming in the integral (1) that $|X - x| \ll |Y - y|$ we can derive the approximate result

$$\alpha = \frac{1}{4\pi}\int_0^1 \frac{l(\xi', y)\, d\xi'}{\xi - \xi'} - \frac{1}{4\pi}\int_{-s}^{s} \frac{\Gamma(Y)\, dY}{(Y - y)^2} \tag{2}$$

$$= \alpha_e(\xi, y) + \alpha_i(y) \tag{3}$$

where ξ is the local section coordinate, given in terms of the leading-edge coordinate $x_L(y)$ and local chord $c(y)$ by

$$x = x_L(y) + c(y)\xi, \tag{4}$$

s is the semi-span and $\Gamma(y)$ is the spanwise vorticity (for a unit incident free stream),

$$\Gamma(y) = \tfrac{1}{2}c(y)\int_0^1 l(\xi, y)\, d\xi. \tag{5}$$

The first term α_e on the right side of (2) is the downwash field due to an infinite straight unsheared wing, with loading l depending only on ξ and having everywhere the chordwise behaviour it actually has at the station y. If this behaviour happens to be the flat-plate type, α_e is independent of ξ and is called the 'effective incidence'.

We remark here, that for a swept wing we can define a mean sweep angle φ at each spanwise station y, and then for large aspect ratio, far from the centre line and the wing tips, the effective incidence in (2) can be multiplied by a factor $\sec \varphi = b(y)$:

$$\alpha_e(\xi, y) = \frac{b(y)}{4\pi}\int_0^1 \frac{l(\xi', y)\, d\xi'}{\xi - \xi'}.$$

The consequences of using this expression in (2) have been partly worked out, and provision made in the computer program for non-zero mean sweep; however, in this Report we shall confine ourselves to the case $\varphi \equiv 0, b \equiv 1$.

The 'induced incidence' α_i is always a function of y only. For an uncambered, but possibly twisted, wing α is also a function of y only, and hence—according to (2)—so is the effective incidence α_e. Then (2) can be regarded as an integral equation for $l(\xi, y)$ with a right side $\alpha - \alpha_i$ independent of ξ, so that l in this case is simply a twist loading:

$$l(\xi, y) = \left(\frac{1 - \xi}{\xi}\right)^{\frac{1}{2}} \frac{4}{\pi c(y)}\Gamma(y). \tag{6}$$

Substituting in (2) for l now gives Prandtl's integral equation for Γ in terms of α:

$$\frac{\Gamma(y)}{\pi c(y)} - \frac{1}{4\pi}\int_{-s}^{s} \frac{\Gamma(Y)\, dY}{(Y - y)^2} = \alpha(y). \tag{7}$$

2.1. The Equivalent Twodimensional Loading

In general α is a function of both x (or ξ) and y, and then (6) has to be modified. The following technique does this approximately for cambered distributions α while reducing to (6) in the uncambered case. We introduce the equivalent twodimensional loading $l_T(\xi; y)$, i.e. the loading which produces the downwash

α on the infinite straight unsheared wing:

$$\alpha(\xi\,;y) = \frac{1}{4\pi}\int_0^1 \frac{l_T(\xi'\,;y)\,d\xi'}{\xi - \xi'}. \tag{8}$$

Since α is given as data, or as a computed downwash difference field after the first iteration, we can obtain the corresponding l_T. The inverse of (8) for each y is

$$l_T(\xi\,;y) = -\frac{4}{\pi}\left(\frac{1-\xi}{\xi}\right)^{\frac{1}{2}}\int_0^1 \left(\frac{\xi'}{1-\xi'}\right)^{\frac{1}{2}}\alpha(\xi'\,;y)\frac{d\xi'}{\xi'-\xi}\,. \tag{9}$$

Changing to the angular chordwise coordinate ϕ where

$$\xi = \tfrac{1}{2}(1 - \cos\phi), \tag{10}$$

we can easily evaluate (9) numerically. The details can be found in Appendix I. The transformation (10) is also convenient later for the downwash evaluation[1,2].

We next compute the equivalent spanwise vorticity, defined similarly to (5):

$$\Gamma_T(y) = \tfrac{1}{2}c(y)\int_0^1 l_T(\xi\,;y)\,d\xi. \tag{11}$$

This equation (11) can now be used to define an 'aerodynamic mean incidence' for cambered wings, for use in the right side of Prandtl's equation (7). Reverting for a moment to the uncambered wing, we see that the solution of (8) for the equivalent twodimensional loading takes the same form as equation (6):

$$l_T(\xi\,;y) = \left(\frac{1-\xi}{\xi}\right)^{\frac{1}{2}}\frac{4}{\pi c(y)}\Gamma_T(y) \tag{12}$$

with

$$\alpha(y) = \frac{\Gamma_T(y)}{\pi c(y)}. \tag{13}$$

So equation (13) can also be used to define the mean incidence when generalizing to the cambered case.

2.2. Prandtl's Integral Equation

We now substitute for $\alpha(y)$ from the generalized equation (13) in equation (7). We also normalize the spanwise variable y to the nondimensional one

$$\eta = y/s. \tag{14}$$

From this point on, all functions of y will be regarded as functions of η. Equation (7) becomes

$$\frac{2s}{\pi c(\eta)}\Gamma(\eta) - \frac{1}{2\pi}\int_{-1}^1 \frac{\Gamma(\eta')\,d\eta'}{(\eta-\eta')^2} = \frac{2s}{\pi c(\eta)}\Gamma_T(\eta). \tag{15}$$

This equation now gives Γ in terms of the known function Γ_T and so generalizes the simple form (7) to cambered wings, as desired. The solution of (15) with $\Gamma(\eta) = 0(\sqrt{1-\eta^2})$ near $\eta = \pm 1$ can be obtained numerically using Multhopp's technique[3], if the spanwise distribution of stations is chosen suitably. Our present choice was influenced by the consideration that enough stations should be available near the wing tips, to be confident of evaluating downwash accurate to 1 per cent there by the Sells method[1,2]; on the other hand, we do not need so many stations for the same job inboard, near the root, and to use more than necessary would be wasteful of computer time and storage. After some experiments, it was decided to employ the '$m = 31$' distribution (in Multhopp's notation) in the inboard region $0 \leqslant \eta \leqslant 0{\cdot}7071$ (8 stations) and the '$m = 63$' distribution, omitting the last one, in the outboard region $0{\cdot}7071 \leqslant \eta < 1$ (15 stations). These stations include the rest of the '$m = 31$' set. It is then sufficiently accurate to iterate (15) to convergence using Multhopp's equations for the complete '$m = 31$' set, and to compute the values of Γ on those '$m = 63$' stations not in the '$m = 31$' set, by using the Multhopp equations for those stations

just once; in matrix terms, these equations show marked diagonal dominance, which increases rapidly with increasing 'm'.

3. Modification of Prandtl's Load Distribution

3.1. Choice of Spanwise Relaxation Factors

Having solved (15) for $\Gamma(\eta)$, we have to compute and store a suitable load distribution for the downwash calculation. For the uncambered wing there is no problem, as the loading is given by (6). In the general case we may re-interpret Prandtl's theory as implying that l is basically the equivalent twodimensional loading l_T less a twist loading contribution due to the trailing vortices (giving rise to the induced incidence):

$$l \approx l_T - 4\left(\frac{1-\xi}{\xi}\right)^{\frac{1}{2}} \alpha_i(\eta). \tag{16}$$

For the uncambered wing, substitution of (12) and use of Prandtl's equation shows that (16) is exactly equivalent to (6). In the general case we may integrate (16) chordwise and see that Prandtl's equation (15) is satisfied, so that the spanwise loading is indeed equal to $\Gamma(\eta)$ and behaves like $\sqrt{1-\eta^2}$ near the tips, but the chord loading l does not itself behave like $\sqrt{1-\eta^2}$ for every ξ, as it should (except perhaps at the LE $\xi = 0$) for a wing with finite tip chord. This would not have troubled Prandtl, as his wings were normally elliptical in planform, his theory is wrong near the tips anyway as the large aspect ratio assumption breaks down, but this for him would have been a comparatively small region and he was more interested in the overall spanwise loading; but it is of concern to us today as we need to know something about the tip chord loading for drag calculations, and it is necessary for the proper calculation of downwash[1,2] near the tips, that the chord loading should fall to zero there—the program assumes the $\sqrt{1-\eta^2}$ behaviour. So equation (16) cannot be used as it stands for the general chord loading.

After much experiment, the following method was adopted. From (3) and (15)

$$\alpha_i = -\frac{1}{4\pi s}\int_{-1}^{1} \frac{\Gamma(\eta')\,d\eta'}{(\eta-\eta')^2}$$

$$= \frac{1}{\pi c(\eta)}[\Gamma_T(\eta) - \Gamma(\eta)]. \tag{17}$$

With the help of (17), equation (16) can be written

$$l = \frac{4}{\pi c(\eta)}\left(\frac{1-\xi}{\xi}\right)^{\frac{1}{2}}\Gamma(\eta) + \left[l_T - \frac{4}{\pi c(\eta)}\left(\frac{1-\xi}{\xi}\right)^{\frac{1}{2}}\Gamma_T(\eta)\right]. \tag{18}$$

The first term on the right side of (18) is a twist loading factored with $\Gamma(\eta)$ which behaves correctly as $\eta \to \pm 1$. We now modify equation (18) by multiplying the second term (in square brackets) by a function $f(\eta)$ which is close to 1 over most of the wing but which is also $0(\sqrt{1-\eta^2})$ near the tips:

$$l = \frac{4}{\pi c(\eta)}\left(\frac{1-\xi}{\xi}\right)^{\frac{1}{2}}\Gamma(\eta) + \left[l_T - \frac{4}{\pi c(\eta)}\left(\frac{1-\xi}{\xi}\right)^{\frac{1}{2}}\Gamma_T(\eta)\right] f(\eta). \tag{19}$$

We remark that for the uncambered wing, by equation (12) the square bracket is zero and (19) reduces to Prandtl's classical solution (6), for any choice of $f(\eta)$.

We can now describe the iteration cycle. The loading (19) is input to the downwash program, which is incorporated as a subroutine, and the downwash field $\alpha^{(1)}(\xi, \eta)$ is calculated. Hence we can derive a difference field

$$\Delta\alpha^{(1)} = \alpha - \alpha^{(1)}.$$

This difference field is input to equation (9) and a correction $\Delta l^{(2)}$ to the loading is calculated and added on to the existing loading. At the nth iteration we calculate a downwash field $\alpha^{(n)}$ and difference field

$$\Delta\alpha^{(n)} = \alpha - \alpha^{(n)}$$

and a loading correction $\Delta l^{(n)}$; and we can repeat this iteration until $\Delta l^{(n)}$ or $\Delta\alpha^{(n)}$ is small enough.

The function $f(\eta)$ is a spanwise relaxation factor, applied to (16) to ensure that l has the right behaviour near the tips. The choice of $f(\eta)$ is at our disposal. By experience we have found that f should be a smoothly varying function even up to the second derivative, otherwise oscillations set in as the iteration proceeds; to keep f close to 1 for much of the span, we tried

$$f(\eta) = \sqrt{1 - \eta^{12}}. \tag{20}$$

For a rectangular wing with parabolic camber, which will be discussed in the results section, this choice of f gave quite a good first guess but as the iterations proceeded, the downwash difference fields developed rapid variations (overshoots) near the mid-chord tips, which suggested that for the highly cambered and twisted difference fields $\Delta\alpha$ after the first, the factor f in (20) was giving too large a change of loading Δl near the tips. The next trial

$$f(\eta) = \sqrt{1 - \eta^4} \tag{21}$$

gave much better convergence near the tip for the complicated cambered difference fields $\Delta\alpha$ after the first, but the difference fields $\Delta\alpha^{(1)}$ first time were larger than those for the choice (20). So the program was arranged to take the choice (20) at the first iteration and (21) thereafter, thereby achieving the advantages of both:

$$f(\eta) = \begin{cases} \sqrt{1 - \eta^{12}} & n = 1 \\ \sqrt{1 - \eta^4} & n \geqslant 2 \end{cases}. \tag{22}$$

There is no special virtue in the exact powers 12 and 4 of η in (22); they were arrived at simply by crude estimates for one case, but are believed to be qualitatively of the right order of magnitude.

3.2. Some Intermediate Results

The method as developed to this point was applied to the problem of calculating the load distribution on an unswept rectangular flat plate of aspect ratio $A = 6$ (so that, with the semi-span $s = 1$, we have the chord $c = \frac{1}{3}$), at unit incidence, so that the data for downwash were: $\alpha(\xi, \eta) \equiv 1$. For this uncambered wing the first iterates (Prandtl's solution) for l_T and l are the flat-plate solutions (12) and (6). This calculation was run for 3 iterations, and the results for the first (Prandtl) and third iterations are plotted, the chordwise loading (in the form $l \sin \phi$ which is finite at the LE $\phi = 0, \xi = 0$) at the wing root (or mid-span station) $\eta = 0$ and also at approximately 90 per cent and 99 per cent semi-span stations in Fig. 1, and the corresponding downwash fields at the same spanwise stations in Fig. 2. The detailed results show that the loading is converging at all points, with some difficulty being found at the leading edge (LE) 99 per cent (near tip) station where the loading is developing a steep chordwise gradient characteristic of small effective aspect ratio. The Prandtl solution is very much in error near the tip, the resulting downwash $\alpha^{(1)}$ being 76 per cent too low at the 99 per cent station LE and 83 per cent too high at the trailing edge (TE—these values are not shown), and at the 90 per cent station the errors are 20 per cent at LE, 36 per cent at TE. However the error at the root is only 4 per cent, as this is where the large aspect ratio approximation (2) is best. After 3 iterations the downwash $\alpha^{(3)}$ at the near-tip station is about 50 per cent too low at LE and 20 per cent too high at TE but inboard of the 90 per cent station the errors are around 1 per cent so that the solution has converged fairly well there.

The tip obviously presents a problem, and to obtain rapid convergence there we should perhaps seek and employ load functions of a different kind, similar to the swept-wing apex eigenfunctions of Rossiter[8]. It is known[5,6] that for local functions of flat-plate type chordwise, and elliptic spanwise, the downwash becomes large and negative, showing a logarithmic singularity as we approach the tip LE, and this explains why the values in this corner are so low. We comment further on this singularity in Appendix II. However, making a rough extrapolation of the results, we find that the loading errors are likely to be small, around 6 per cent of the root loading, and confined to this corner region—apart from a small sub-

region, very near the actual sharp corner itself, where the loading takes on a different character and nothing can be said about its actual magnitude in this work.

The method as so far described, although it has been shown to converge for the rectangular flat-plate problem is not entirely attractive. Each iteration requires a downwash field calculation; using our 23×8 mesh, the downwash at one point takes 4 seconds of central processor time to evaluate on an ICL 1907, and so even calculating the downwash only at every third station spanwise starting from the centre line, that is to say at 8 spanwise stations, with 9 chordwise points at each station the downwash field computation takes around 300 central processor seconds. If one is satisfied with the final answer on inspection, one need not of course do the last downwash field calculation, but it has been incorporated in the test program during development, as a check. Perhaps during the later stages it would be possible to calculate the downwash at only one or two sections near the tip, leaving the inboard loading to look after itself, but this might need care to avoid forming waves where the new perturbed loading is faired into the inboard loading, as downwash calculations are very sensitive to the smoothness of the loading data. Routines have in fact been incorporated to ensure spanwise smoothness outboard of the equivalent two-dimensional loading, and also to interpolate for it after calculating it from the downwash difference field computed at every third station, so this might not be too difficult. However, we should seek a refinement of the method which gives a better first approximation than Prandtl's overall, so that the first downwash difference field to be cancelled is small, as then greater accuracy would be obtained, or fewer downwash calculations and less computer time for the same accuracy, would be needed. Such a refinement has been evolved, and will be described next.

4. Weber's Conjecture

We have seen in the results of the previous section that for a given load distribution the downwash predicted by Prandtl's theory, equation (2), near the tip tends to be too high at the leading edge and too low at the trailing edge, compared with the true downwash, and behaves monotonically between these limits chordwise; the discrepancy decreases as we proceed inboard. Similar results have been obtained for some other loading distributions (the first and second Birnbaum chordwise distributions with elliptic spanwise variation have been tried) and with a 45 degree swept constant-chord wing, also of aspect ratio 6. Of course, the observance of this behaviour for these cases does not prove that this behaviour always obtains, and the tip leading edge behaviour is surely the effect of the logarithmic singularity discovered by Ray and Miller[5] for rectangular wings; one would expect a similar effect for swept wings. However, we propose to incorporate something of this behaviour in an iteration scheme and see if this gives an improvement on Prandtl's theory.

We need to place this tendency on a quantitative basis, which need not be very accurate as it is only a conjecture, and moreover intended for iteration. Weber[7] has analysed the computed downwash fields for the above-mentioned wings and loading distributions, and she finds that over most of the wing, $0{\cdot}1 \leqslant \eta \leqslant 0{\cdot}9$ say,

$$\alpha \doteq \alpha_e + \alpha_i + h(\xi)k(\eta)\alpha_i. \tag{23}$$

The function $h(\xi)$ takes care of the chordwise variation and takes negative values near the LE $\xi = 0$ and positive values near the TE; we can take

$$h(\xi) = -0{\cdot}5 + 2{\cdot}5\xi - \xi^2. \tag{24}$$

The function $k(\eta)$ accounts for the spanwise variation and is to be small near the root $\eta = 0$ and around unity near the tip $\eta = 1$; we can take

$$k(\eta) = \frac{1}{1 + 6(1 - |\eta|)} = \frac{1}{7 - 6|\eta|} \tag{25}$$

which might perhaps be generalized later to

$$k(\eta) = \frac{1}{1 + A(1 - |\eta|)}$$

for arbitrary aspect ratio A.

Equation (23) then says that the true downwash differs from that which Prandtl's theory would imply for that load distribution by the product of a chordwise factor, a spanwise factor, and the induced incidence $\alpha_i(\eta)$ which also depends only on η. This equation still does not properly represent the logarithmic singularity in α at the tip LE, but if we tried to account for this local singularity the following simple treatment would break down. We now apply Prandtl's method (implicitly, since $\alpha_i(\eta)$ is not known yet) to that part of the downwash which would be predicted by his theory, namely the part

$$\alpha_e(\xi, \eta) + \alpha_i(\eta) = \alpha - h(\xi)k(\eta)\alpha_i(\eta). \tag{26}$$

For the rest of the description we shall omit superscripts (iteration numbers) and prefixes Δ, as it is obvious how to apply the equations to the difference downwash fields in subsequent iterations.

Let us distinguish the quantities which arise from Prandtl's treatment of the right side of (26) by a tilde, thus the equivalent twodimensional loading $\tilde{l}_T$ satisfies the integral equation (8) with α replaced by the right side of (26). Similarly to (9), the solution of this equation for $\tilde{l}_T$ reads:

$$\tilde{l}_T(\xi\,;\eta) = \frac{4}{\pi}\left(\frac{1-\xi}{\xi}\right)^{\frac{1}{2}} \int_0^1 \left(\frac{\xi'}{1-\xi'}\right)^{\frac{1}{2}} [\alpha(\xi'\,;\eta) - h(\xi')k(\eta)\alpha_i(\eta)] \frac{d\xi'}{\xi' - \xi}.$$

Making use of (9), this becomes

$$\tilde{l}_T(\xi\,;\eta) = l_T(\xi\,;\eta) - H(\xi)k(\eta)\alpha_i(\eta) \tag{27}$$

where $H(\xi)$ is the equivalent twodimensional loading corresponding to $h(\xi)$ in (24), viz.

$$H(\xi) = \tfrac{3}{2}\sqrt{1/\xi - 1} + 6\sqrt{\xi(1-\xi)} + 2(1-2\xi)\sqrt{\xi(1-\xi)}. \tag{28}$$

The corresponding equivalent spanwise vorticity is found by integration as in (11), and is

$$\tilde{\Gamma}_T(\eta) = \Gamma_T - \tfrac{3}{4}\pi c(\eta)k(\eta)\alpha_i(\eta). \tag{29}$$

Corresponding to (15), Prandtl's equation for the spanwise vorticity $\tilde{\Gamma}(\eta)$ reads:

$$\begin{aligned}\frac{2s}{\pi c(\eta)}\tilde{\Gamma}(\eta) - \frac{1}{2\pi}\int_{-1}^{1} \frac{\tilde{\Gamma}(\eta')\,d\eta'}{(\eta - \eta')^2} &= \frac{2s}{\pi c(\eta)}\tilde{\Gamma}_T(\eta) \\ &= \frac{2s}{\pi c(\eta)}\Gamma_T(\eta) - \tfrac{3}{2}sk(\eta)\alpha_i(\eta).\end{aligned} \tag{30}$$

From the definition of induced incidence, the analogue of (3) is

$$\alpha_i(\eta) = -\frac{1}{4\pi s}\int_{-1}^{1} \frac{\tilde{\Gamma}(\eta')\,d\eta'}{(\eta - \eta')^2} \tag{31}$$

Substituting for α_i in (30) and rearranging:

$$\frac{2s/\pi c(\eta)}{1 + \frac{3}{4}k(\eta)}\tilde{\Gamma}(\eta) - \frac{1}{2\pi}\int_{-1}^{1} \frac{\tilde{\Gamma}(\eta')\,d\eta'}{(\eta - \eta')^2} = \frac{2s/\pi c(\eta)}{1 + \frac{3}{4}k(\eta)}\Gamma_T(\eta). \tag{32}$$

We see at once that this is a simple modified form of Prandtl's equation (15) in which the two terms not involving the integral are factored by $[1 + \frac{3}{4}k(\eta)]^{-1}$. Having computed l_T and Γ_T in exactly the same way as before, the program modification to Multhopp's scheme is trivial.

When $\tilde{\Gamma}(\eta)$ has been determined, $\alpha_i(\eta)$ follows from (31), $\tilde{\Gamma}_T$ from (29), $\tilde{l}_T$ from (27) and $\tilde{l}(\xi\,;\eta)$ from the analogue of (16):

$$\tilde{l} \approx \tilde{l}_T - 4\left(\frac{1-\xi}{\xi}\right)^{\frac{1}{2}} \alpha_i(\eta).$$

Making use of (30) and (31), this is rearranged as in (18) and the factor $f(\eta)$ is added as in (19):

$$\tilde{l} = \frac{4}{\pi c(\eta)}\left(\frac{1-\xi}{\xi}\right)^{\frac{1}{2}} \tilde{\Gamma}(\eta) + \left[\tilde{l}_T - \frac{4}{\pi c(\eta)}\left(\frac{1-\xi}{\xi}\right)^{\frac{1}{2}} \tilde{\Gamma}_T(\eta)\right] f(\eta). \tag{33}$$

We observe that the square bracket would again vanish if $\tilde{l}_T$ happened to be a twist loading, making the choice of $f(\eta)$ immaterial, but that even when this is not so, the loading $\tilde{l}$ still behaves suitably for $\eta \to \pm 1$, since both terms do so if $f(\eta)$ is chosen as before, viz. (22).

The downwash difference field can now be computed and the iteration restarted as desired.

5. Results

5.1. Flat-Plate Wing

This method, refined with the aid of Section 4, has been tried on the same wing as before, the rectangular wing of aspect ratio 6 at unit incidence. Three iterations were run, and the results (spanwise vorticity, chordwise loading and percentage downwash error) are shown in Figs. 3, 4, 5 respectively. We observe at once that the first guess for the loading is much closer to the correct answer than the Prandtl solution in the previous run (*see* Figs. 1 and 2); analysing the downwash field in detail, at the 99 per cent (near-tip) station the error is 58 per cent at the LE (not shown) but only 18 per cent too high at the TE, so while the new conjecture has been unable to improve matters very near the logarithmic singularity in the corner, the improvement at the TE is remarkable, the error being less than $\frac{1}{4}$ the Prandtl error. Proceeding inboard, at the 90 per cent station the errors are 7 per cent and 6 per cent respectively, the good TE recovery continuing and accompanied by good LE recovery; at the root, the downwash is correct to within 1 per cent except just near the TE, again a substantial improvement on the Prandtl solution. At the second iteration, the root downwash is virtually exact, and that at the 90 per cent station nearly so aft of 30 per cent chord. The only perceptible change in the overall loading between the second and third iterations, occurs in the first 30 per cent chord of the last few spanwise stations near the tip, and this change is shown in Fig. 4, well illustrating the chordwise steepening due to small effective aspect ratio there. At the third iteration, the downwash is within 1 per cent of the target everywhere except near the LE corner and out along the tip to 70 per cent chord; at 90 per cent station LE the error is 2 per cent and at 99 per cent it is 38 per cent. Moreover, the changes in downwash error here from one iteration to another are due to small changes in a comparatively low-loading region; Table 1 shows how the load function and downwash have changed on the LE near the tip, from the second to the third iteration.

Extrapolating these figures roughly to unit downwash, we can expect a percentage error (compared with the root LE load function, which is 6·4668) of about 2 per cent at 90 per cent semi-span, and perhaps 6 per cent at 99 per cent semi-span. We can therefore hope that such things as overall lift and drag will be well predicted by the method. Indeed, from Fig. 3 we see that there is no appreciable difference between the last two iterations for the spanwise vorticity (which is connected to the spanwise lift coefficient by a factor $\frac{1}{2}c$), even when the differences are accentuated by plotting against $\sqrt{1-\eta^2}$. Thus, if we were only interested in this quantity, we could do just two iterations (two loading calculations and one downwash field calculation). The final spanwise vorticity is plotted again in the usual way in Fig. 6, along with the centre of pressure x_{cp} which starts near the infinite flat-plate position 0·25 at the root and moves forward as we approach the wing tip and the chordwise LE loading steepens. The complete results for the load function and downwash field (check calculation) are reproduced in Table 2.

In Table 3 we compare our solution with the solution obtained by a collocation method[9], and communicated privately by Garner. To avoid interpolation, only the results at the stations common to both calculations are shown. From the table we see that the two calculations differ in the third significant figure as a rule, thus agreeing to 1 per cent or better, with particularly good agreement in centre of pressure x_{cp}. Garner's value of load function is higher than ours at the LE near the tip ($\eta = 0{\cdot}9239$), as it should be to get the downwash up, in that corner. This generally good agreement augurs well for our calculation method, with 23 points across the semi-span but only 8 across the chord.

5.2. Parabolic Camber Wing

To demonstrate the efficiency of the program on a cambered wing, the rectangular wing of aspect ratio 6 was again considered with a datum downwash field

$$\alpha(\xi) = 2\xi - 1$$

which implies a parabolic camber line

$$z = \frac{x}{c}\left(1 - \frac{x}{c}\right).$$

As before, three iterations were run, and the iterates for spanwise vorticity, chordwise loading and downwash error are shown in Figs. 7, 8 and 9. The convergence trends are very similar to those for the flat plate in the last subsection; the spanwise vorticity has effectively converged after 2 iterations, the chordwise loading is not noticeably changed between the second and third iterations in the figure and the steepening near the tip LE is apparent as the iterations proceed (the steepening at the second iteration is not shown, for the sake of clarity). Since the tip LE chordwise loading has come out negative, the downwash singularity in this corner has opposite sign, and in Fig. 9 we indeed find a large positive downwash at first in this corner, the error at the 99 per cent LE station being 57 per cent at the first iteration (not shown) but reducing to 30 per cent at the third iteration. Qualitatively the errors in the field behave very similarly to those in the flat-plate case, the overall downwash field at the end being accurate to better than 1 per cent, with slight excesses near the LE corner and down the tip. Our results are compared with those due to Garner[9] in Table 4, and again the differences are in the third significant figure, with excellent agreement in centre of pressure (which would have a value of 0·5 for the infinite cambered wing, but for our finite wing starts just aft of this at the root and moves still further aft as we approach the tip, *see* also Fig. 10). The complete results for loading function, and final check downwash field calculation, are displayed in Table 5.

It may be that further improvement is obtained by better choice of the relaxation function f in (33), the combination (22) being the only one we have tried (having explained our reasons for choosing a combination in Section 3), or by better choice of the Weber conjecture functions $h(\xi)$ and $k(\eta)$ in (23). The program has been written in such a way that the modifications would be trivial. But this would need care. Looking at Figs. 5 and 9, we see that near the tip LE the downwash is slowly converging monotonically to the desired value, but that near the tip TE the downwash converges by oscillation for the flat plate but monotonically for the parabolic camber wing. In view of this sensitive behaviour, it is unlikely that any optima for these cases would be universal optima for all wings, and certain other aspects more urgently await consideration, so we leave this question open awhile and rest content with having found a partial solution to the special problems presented by a rectangular tip.

6. Conclusion

By incorporating a relaxation scheme for the chordwise loading into Prandtl's theory, and making use of a conjecture of Weber[7] concerning the difference between the exact downwash and that which would be expected from Prandtl's theory for the same loading, we have developed a pilot method to calculate the loading iteratively on a thin wing with prescribed warp (downwash). The method has been tested on a rectangular flat-plate wing of aspect ratio 6 at incidence, and also on a cambered wing with the same planform; for the traditional types of load distribution the downwash shows a logarithmic infinity as we approach the leading-edge tip, and this means in practice that there is a small region near this corner where convergence is severely retarded—it never could converge exactly at the corner; however, good convergence is obtained elsewhere on the wing, 3 iterations and 2 downwash field calculations being sufficient and needing the reasonable time of 600 central processor seconds (about 15 minutes) on an ICL 1907 computer. That the results are good, has been confirmed in both cases by a third downwash calculation using the final load distribution, as a check, the downwash away from the critical corner being accurate to within 1 per cent. Apart from the very tip corner itself, where the loading must have a different asymptotic character from that assumed, the error in loading in the small corner region is estimated at around 6 per cent of the mid-span loading, and so is unlikely to affect overall properties seriously. Good local and overall agreement is found in comparisons with results[9] communicated by Garner.

There still remains the problem of a wing with centre line sweep. Unless a very fine mesh is taken near the centre line of such a wing, the downwash calculation by the method of Ref. 2 is liable to have large errors there, and it is probably necessary to treat the apex properly by considering the eigensolutions of Rossiter[8], before we can establish a viable method for this case. For this reason our method is regarded as a pilot method only, awaiting further development.

Acknowledgment. The author gratefully acknowledges many helpful conversations with Dr. J. Weber.

LIST OF SYMBOLS

A	Aspect ratio
$c(\eta)$	Chord
$C_L(\eta)$	Section lift coefficient
e	Load function, $l \sin \phi$
$f, f^{(n)}$	Relaxation factor in modified Prandtl loading
$F(\phi)$	$\alpha(\xi'; y)$ in Appendix I
$h(\xi)$	Chordwise factor of α_i in Weber's conjecture
$H(\xi)$	Twodimensional loading corresponding to $h(\xi)$
$k(\eta)$	Spanwise factor of α_i in Weber's conjecture
l	Loading
n	Iteration number
s	Semi-span
x, X	Downstream cartesian coordinates
y, Y	Spanwise cartesian coordinates
α	Required downwash, given as data
α_e	Twodimensional downwash corresponding to section loading l; 'Effective incidence'
α_i	Induced incidence
$\Gamma(\eta)$	Spanwise vorticity, $\frac{1}{2}cC_L$
ϕ	Angular chordwise coordinate
ξ	Normalized chordwise coordinate $0 \leqslant \xi \leqslant 1$
η	Normalized spanwise coordinate y/s
Prefix Δ	Perturbation quantities (iterative corrections)
Subscript T	Equivalent twodimensional quantities

Superscripts

(n)	Quantities at nth iteration
$\sim$	Quantities found using Weber's conjecture

REFERENCES

No.	*Author*	*Title, etc.*
1	C. C. L. Sells	Calculation of the induced downwash field on and off the wing plane for a wing with given load distribution. R.A.E. Technical Report 69231 (ARC 32144) (1969).
2	C. C. L. Sells	Calculation of the downwash on the centre line of a swept wing with given load distribution. A.R.C. 32549, R.A.E. Technical Report 70146 (1970).
3	H. Multhopp	Methods for calculating the lift distribution of wings (subsonic lifting surface theory). A.R.C. R. & M. 2884 (1950).
4	B. Thwaites	*Incompressible aerodynamics.* Chapter VIII. Clarendon Press (1960).
5	Valerie A. Ray and G. F. Miller	Numerical evaluation of the downwash integral for a lifting rectangular planform. NPL Report Math 90 (1970).
6	H. C. Garner and G. F. Miller	Analytical and numerical studies of downwash over rectangular planforms. *The Aero Quarterly, Vol. XXIII, Part 3,* pp. 169–180, August 1972.
7	J. Weber	Notes on the approximate solution of lifting-surface theory used in the RAE Standard Method.
8	Patricia J. Rossiter	The linearized subsonic flow over the centre section of a lifting swept wing. A.R.C. R. & M. 3630 (1970).
9	D. E. Lehrian and H. C. Garner	Theoretical calculation of generalized forces and load distribution on wings oscillating at general frequency in a subsonic stream. A.R.C. R. & M. 3710, 1971.

APPENDIX I

Calculation of Equivalent Twodimensional Loading

We have to evaluate equation (9) for l_T:

$$l_T(\xi; y) = \frac{4}{\pi}\left(\frac{1-\xi}{\xi}\right)^{\frac{1}{2}} \int_0^1 \left(\frac{\xi'}{1-\xi'}\right)^{\frac{1}{2}} \alpha(\xi'; y) \frac{d\xi'}{\xi' - \xi} \tag{I.1}$$

when data for α are available at a reasonable number of chordwise stations for each y (currently, 8 chordwise intervals are used, giving 9 stations including leading and trailing edges). We transform the chordwise coordinate ξ to the angular coordinate ϕ by

$$\xi = \tfrac{1}{2}(1 - \cos\phi) \tag{I.2}$$

and the integrating variable similarly by

$$\xi' = \tfrac{1}{2}(1 - \cos\theta). \tag{I.3}$$

Also, in the computation we work with the load function

$$e_T = l_T \sin\phi, \tag{I.4}$$

which is well-behaved at LE and TE, although in the text we refer principally to the loading. Since we also employ

$$e = l \sin\phi \tag{I.5}$$

to calculate[1,2] the downwash from each loading iterate, the same linear combinations work for e and e_T as for l and l_T in the main text.

We write also

$$\alpha(\xi'; y) = F(\theta).$$

Equation (I.1) becomes

$$e_T(\phi; y) = \frac{4}{\pi}(1 + \cos\phi) \int_0^\pi F(\theta)\, d\theta \frac{1 - \cos\theta}{\cos\phi - \cos\theta}. \tag{I.6}$$

The integral is recast in standard finite form:

$$e_T(\phi; y) = \frac{4}{\pi}(1 + \cos\phi)\left[\int_0^\pi \frac{d\theta}{\cos\phi - \cos\theta}\{(1 - \cos\theta)F(\theta) - (1 - \cos\phi)F(\phi)\}\right.$$
$$\left. + (1 - \cos\phi)F(\phi) \int_0^\pi \frac{d\theta}{\cos\phi - \cos\theta}\right]. \tag{I.7}$$

The last integral is zero. By L'Hospital's rule, the limit of the integrand at $\theta = \phi$ is

$$\lim_{\theta \to \phi} \frac{d[(1 - \cos\theta)F(\theta)]/d\theta}{d(\cos\phi - \cos\theta)/d\theta} = F(\phi) + \tan\frac{\phi}{2} F'(\phi).$$

This breaks down at $\phi = \pi$, but because of the factor $(1 + \cos\phi)$, e_T (and l_T) are both zero at $\phi = \pi$ (i.e. $\xi = 1$, the trailing edge) anyway. With a difference approximation for $F'(\phi)$, $e_T(\phi; y)$ can be calculated from (I.7) by the trapezoidal rule. For computing efficiency, we write the denominator

$$\cos\phi - \cos\theta = 2\sin\frac{\theta + \phi}{2}\sin\frac{\theta - \phi}{2}$$

and store cosec $(\theta/2)$ before entering the subroutine; this replaces each division by two multiplications and saves computer time.

In this way we obtain the equivalent twodimensional loading at each spanwise section, in the form $l_T \sin\phi = e_T$. e_T is finite right up to the leading edge, where its value is also needed later, to form e as in (I.5) for the downwash calculation. For an unyawed flat-plate, for example, the downwash field $\alpha(x, y) \equiv 1$ gives an equivalent twodimensional loading

$$l_T(\xi) = 4\sqrt{\frac{(1 - \xi)}{\xi}},$$

whence

$$e_T = 4(1 + \cos\phi).$$

Moreover, having evaluated (I.7) we may compute the equivalent spanwise vorticity

$$\Gamma_T(y) = \tfrac{1}{2}c(y)C_{LT}(y)$$

where

$$C_{LT} = \int_0^1 l_T(\xi; y)\, d\xi$$

$$= \int_0^\pi l_T \cdot \tfrac{1}{2}\sin\phi\, d\phi = \tfrac{1}{2}\int_0^\pi e_T\, d\phi.$$

For the example above

$$C_{LT} = 2\pi.$$

APPENDIX II

The Corner Singularity in Downwash

It has been shown[5,6] that for a rectangular wing with chord c and aspect ratio A, under the flat-plate elliptic loading

$$l = K(1/\xi - 1)^{\frac{1}{2}}(1 - \eta^2)^{\frac{1}{2}}, \tag{II.1}$$

the downwash exhibits a logarithmic singularity near the tip LE:

$$\alpha \sim K\frac{0{\cdot}1349}{A^{\frac{1}{2}}} \ln (r/c), \tag{II.2}$$

where r is the distance from the corner, *see* Fig. 11. Now, the Prandtl solution has flat-plate chordwise loading and a reasonable resemblance to elliptic spanwise loading locally, and so we may enquire how well our computed downwash fits the theory.

We may determine K as follows. On the LE $\xi = 0$, $\phi = 0$, and from (II.1)

$$l \sin \phi = 2K(1 - \eta^2)^{\frac{1}{2}}.$$

At the 99 per cent station, $\eta = 0{\cdot}9892$, our results from the intermediate method give

$$l \sin \phi = 1{\cdot}6693$$

whence

$$K = 5{\cdot}6895.$$

Ray and Miller[5] give results for much smaller values of r/c than we encounter, from 10^{-2} down to 10^{-7}, whereas our smallest value of r/c occurs at the 99 per cent section LE and is 0·0324 ($r = 0{\cdot}0108$, $c = \frac{1}{3}$). Substituting this in (I.2) with our aspect ratio $A = 6$, we have

$$\alpha \sim -1{\cdot}0746.$$

The value computed by the program is 0·2427, which we expect to be accurate to about 0·01 with our mesh, so it is clear that the higher order terms in the asymptotic form (II.2) are becoming important, at this comparatively large value of r/c, and we would still less expect good agreement further away from the corner. However, we also have from (II.2)

$$\frac{\partial \alpha}{\partial(\log_{10} r/c)} \sim K\frac{0{\cdot}1349}{A^{\frac{1}{2}}}(2{\cdot}3026)$$
$$= 0{\cdot}7214.$$

So there might possibly be a tendency for α to vary in this way as we recede from the corner. In Fig. 11 we plot α against r on a logarithmic scale, and while there is a certain amount of scatter which we may attribute to the higher order terms in (II.2), the points are indeed distributed about a mean dotted line with the expected slope. (In accordance with good statistical practice, we list the values of α used in Table 6 and the corresponding values of r in Table 7.) It is also evident from Fig. 11 that the direction in which we leave the corner is becoming important; the variation is stronger along the LE, not so strong downstream along the chord.

From this work, we see that the singularity (II.2) still has a strong influence, and we expect such a singularity in linear theory whenever the loading exhibits such a flat-plate component near the tip.

TABLE 1

Iterates on LE near Tip

η	$l^{(2)} \sin \phi$	$\alpha^{(2)}$	$l^{(3)} \sin \phi$	$\alpha^{(3)}$
0·9040	4·1312	0·9573	4·1676	0·9818
0·9892	1·8146	0·4918	1·9405	0·6144

Y	Table of $l \sin \phi$							
0·0000	6·4668	6·2016	5·4584	4·3689	3·1165	1·9019	0·8899	0·2320
0·0980	6·4560	6·1902	5·4458	4·3570	3·1067	1·8949	0·8864	0·2310
0·1951	6·4170	6·1516	5·4083	4·3245	3·0818	1·8778	0·8781	0·2286
0·2903	6·3515	6·0864	5·3446	4·2676	3·0367	1·8472	0·8631	0·2246
0·3827	6·2573	5·9923	5·2527	4·1838	2·9692	1·8014	0·8404	0·2185
0·4714	6·1300	5·8648	5·1275	4·0689	2·8762	1·7389	0·8094	0·2102
0·5556	5·9683	5·7013	4·9634	3·9161	2·7524	1·6566	0·7693	0·1995
0·6344	5·7645	5·4954	4·7567	3·7223	2·5939	1·5510	0·7176	0·1857
0·7071	5·5149	5·2412	4·4980	3·4789	2·3965	1·4212	0·6549	0·1690
0·7410	5·3720	5·0938	4·3449	3·3346	2·2814	1·3473	0·6199	0·1598
0·7730	5·2136	4·9313	4·1773	3·1762	2·1547	1·2662	0·5815	0·1498
0·8032	5·0397	4·7525	3·9929	3·0030	2·0173	1·1786	0·5403	0·1391
0·8315	4·8522	4·5557	3·7847	2·8099	1·8696	1·0877	0·4984	0·1283
0·8577	4·6434	4·3402	3·5607	2·6018	1·7108	0·9904	0·4538	0·1170
0·8819	4·4131	4·1022	3·3153	2·3791	1·5443	0·8896	0·4078	0·1053
0·9040	4·1676	3·8369	3·0347	2·1375	1·3764	0·7930	0·3649	0·0945
0·9239	3·8801	3·5471	2·7379	1·8833	1·2057	0·6980	0·3236	0·0842
0·9415	3·5749	3·2219	2·4112	1·6231	1·0370	0·6046	0·2826	0·0739
0·9569	3·2420	2·8597	2·0649	1·3654	0·8710	0·5102	0·2401	0·0632
0·9700	2·8658	2·4619	1·7089	1·1139	0·7095	0·4165	0·1969	0·0522
0·9808	2·4353	2·0282	1·3482	0·8704	0·5543	0·3252	0·1542	0·0412
0·9892	1·9405	1·5606	0·9895	0·6367	0·4063	0·2379	0·1128	0·0304
0·9952	1·3695	1·0661	0·6445	0·4133	0·2643	0·1544	0·0733	0·0200

Y	X = 0·0000	0·0381	0·1464	0·3087	0·5000	0·6913	0·8536	0·9619	1·0000
0·0000	1·0000	0·9994	1·0001	0·9991	1·0001	0·9995	0·9997	1·0005	0·9987
0·2903	1·0003	0·9998	1·0003	1·0000	1·0003	1·0003	1·0002	1·0008	0·9990
0·5556	1·0001	0·9996	1·0001	0·9997	1·0000	1·0000	1·0000	1·0005	0·9991
0·7410	0·9994	0·9989	0·9998	0·9997	1·0002	1·0002	1·0000	1·0004	0·9994
0·8315	0·9964	0·9962	0·9987	0·9997	1·0009	1·0005	1·0001	1·0003	0·9995
0·9040	0·9818	0·9862	0·9974	1·0069	1·0077	1·0035	1·0001	0·9991	0·9980
0·9569	0·9095	0·9356	0·9899	1·0025	0·9963	0·9941	0·9952	0·9963	0·9950
0·9892	0·6144	0·8503	1·0418	1·0447	1·0313	1·0186	1·0087	1·0021	0·9981

TABLE 3

Comparison with Results from Garner's Method for Flat-plate Rectangular Wing, $A = 6$. $\alpha(x) = 1$

η		$l \sin \phi$ $x = 0$	$l \sin \phi$ $x = 0{\cdot}5$	C_L	x_{cp}
0	Sells	6·4668	3·1165	4·9884	0·2456
	Garner	6·4545	3·1297	4·9950	0·2461
0·3827	S	6·2573	2·9692	4·7886	0·2438
	G	6·2475	2·9766	4·7942	0·2442
0·7071	S	5·5149	2·3965	4·0488	0·2344
	G	5·5122	2·4013	4·0538	0·2348
0·9239	S	3·8801	1·2057	2·4408	0·2059
	G	3·9352	1·2113	2·4427	0·2062

TABLE 4

Comparison with Results from Garner's Method for Parabolic Camber Rectangular Wing, $A = 6$. $\alpha(x) = 2x - 1$

η		$l \sin \phi$ $x = 0$	$l \sin \phi$ $x = 0{\cdot}5$	C_L	x_{cp}
0	Sells	−0·7185	3·6277	2·5480	0·5555
	Garner	−0·7166	3·5915	2·5373	0·5552
0·3827	S	−0·8016	3·5617	2·4637	0·5641
	G	−0·8012	3·5267	2·4535	0·5641
0·7071	S	−1·0625	3·2904	2·1543	0·5967
	G	−1·0702	3·2640	2·1470	0·5975
0·9239	S	−1·2727	2·3893	1·4196	0·6655
	G	−1·3340	2·3707	1·4189	0·6666

TABLE 5

Final Load Function and Downwash Field Iterates for Parabolic Camber Rectangular Wing, $A = 6$

Y	Table of $l \sin \phi$								
0·0000	−0·7185	−0·1386	1·3740	2·9019	3·6277	3·1790	1·8845	0·5267	
0·0980	−0·7230	−0·1434	1·3688	2·8966	3·6231	3·1759	1·8830	0·5263	
0·1951	−0·7390	−0·1594	1·3535	2·8827	3·6119	3·1682	1·8792	0·5253	
0·2903	−0·7652	−0·1854	1·3280	2·8591	3·5920	3·1543	1·8720	0·5234	
0·3827	−0·8016	−0·2223	1·2902	2·8230	3.5617	3·1334	1·8611	0·5206	
0·4714	−0·8507	−0·2719	1·2392	2·7741	3·5201	3·1045	1·8460	0·5168	
0·5556	−0·9141	−0·3346	1·1764	2·7129	3·4655	3·0650	1·8253	0·5117	
0·6344	−0·9822	−0·4048	1·0993	2·6316	3·3897	3·0083	1·7947	0·5040	
0·7071	−1·0625	−0·4874	1·0065	2·5296	3·2904	2·9326	1·7541	0·4941	
0·7410	−1·1098	−0·5346	0·9549	2·4712	3·2307	2·8861	1·7295	0·4882	
0·7730	−1·1522	−0·5791	0·9005	2·4045	3·1592	2·8290	1·6989	0·4807	
0·8032	−1·1881	−0·6193	0·8440	2·3283	3·0741	2·7596	1·6612	0·4712	
0·8315	−1·2296	−0·6625	0·7857	2·2455	2·9775	2·6797	1·6181	0·4610	
0·8577	−1·2579	−0·6961	0·7273	2·1509	2·8618	2·5817	1·5638	0·4478	
0·8819	−1·2710	−0·7184	0·6684	2·0425	2·7246	2·4638	1·4976	0·4313	
0·9040	−1·2850	−0·7391	0·6083	1·9228	2·5697	2·3299	1·4237	0·4135	
0·9239	−1·2727	−0·7444	0·5460	1·7854	2·3893	2·1729	1·3356	0·3912	
0·9415	−1·2307	−0·7275	0·4843	1·6283	2·1798	1·9881	1·2299	0·3635	
0·9569	−1·1751	−0·6933	0·4255	1·4540	1·9436	1·7769	1·1076	0·3321	
0·9700	−1·0878	−0·6350	0·3673	1·2595	1·6785	1·5372	0·9662	0·2948	
0·9808	−0·9479	−0·5460	0·3059	1·0415	1·3827	1·2680	0·8031	0·2491	
0·9892	−0·7564	−0·4295	0·2391	0·8018	1·0599	0·9729	0·6204	0·1951	
0·9952	−0·5346	−0·2997	0·1659	0·5480	0·7214	0·6628	0·4254	0·1356	

Y	$X = 0·0000$	0·0381	0·1464	0·3087	0·5000	0·6913	0·8536	0·9619	1·0000
0·0000	−1·0049	−0·9202	−0·7089	−0·3824	−0·0002	0·3822	0·7087	0·9201	1·0044
0·2903	−1·0045	−0·9199	−0·7087	−0·3822	0·0001	0·3824	0·7089	0·9235	1·0045
0·5556	−1·0051	−0·9199	−0·7086	−0·3823	0·0002	0·3826	0·7091	0·9210	1·0051
0·7410	−1·0053	−0·9178	−0·7071	−0·3816	0·0005	0·3827	0·7086	0·9199	1·0056
0·8315	−1·0036	−0·9134	−0·7050	−0·3821	−0·0008	0·3818	0·7073	0·9200	1·0062
0·9040	−0·9878	−0·8942	−0·6947	−0·3795	0·0003	0·3836	0·7072	0·9157	1·0059
0·9569	−0·9200	−0·8417	−0·6891	−0·3982	−0·0172	0·3761	0·7054	0·9106	0·9986
0·9892	−0·6978	−0·7242	−0·6718	−0·4017	−0·0193	0·3780	0·7082	0·9035	0·9729

TABLE 6

Downwash near LE Corner from Prandtl Loading

η \ ξ	0·0000	0·0381	0·1464	0·3087
0·8315	0·8885			
0·9040	0·8028	0·8420		
0·9569	0·6308	0·7184	0·9281	
0·9892	0·2427	0·5174	0·9483	1·2921

TABLE 7

Corresponding Values of r

η \ ξ	0·0000	0·0381	0·1464	0·3087
0·8315	0·1685			
0·9040	0·0960	0·0968		
0·9569	0·0431	0·0449	0·0651	
0·9892	0·0108	0·0167	0·0500	0·1035

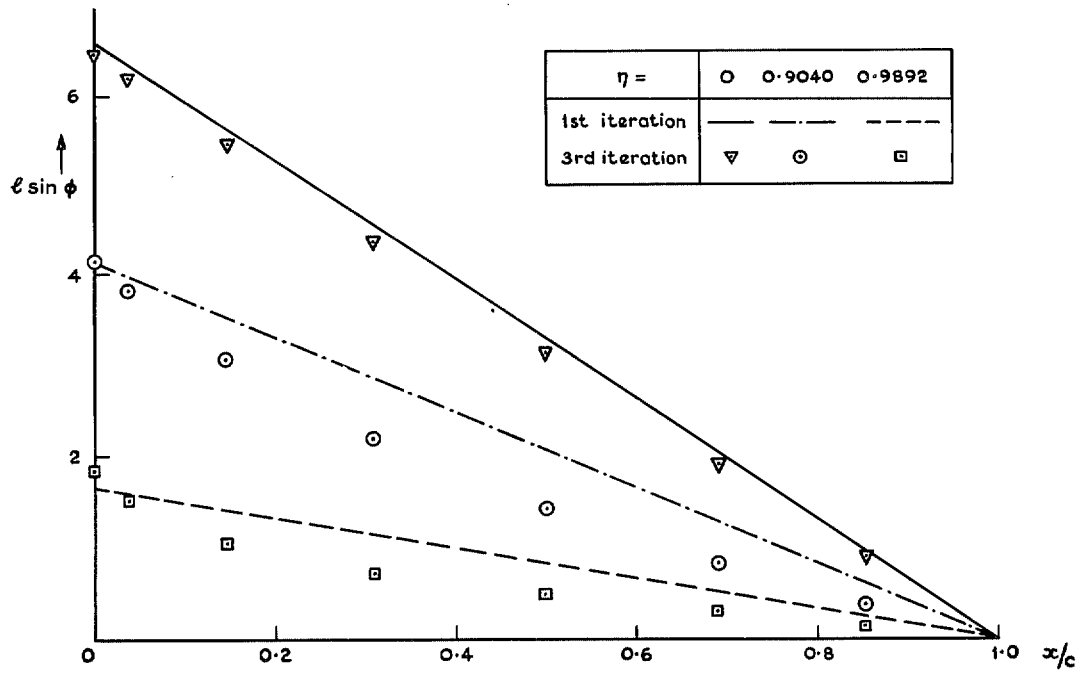

FIG. 1. Chordwise loading iterates from intermediate method for flat-plate rectangular wing, $A = 6$.

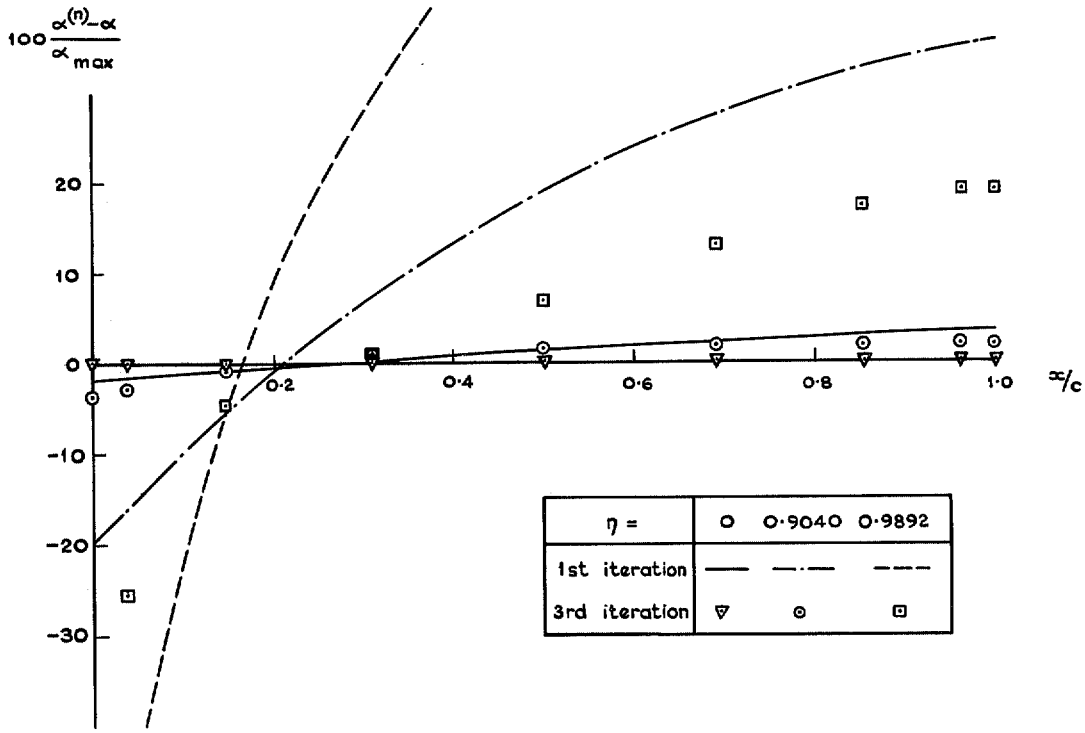

FIG. 2. Percentage downwash error iterates from intermediate method for flat-plate rectangular wing, $A = 6$.

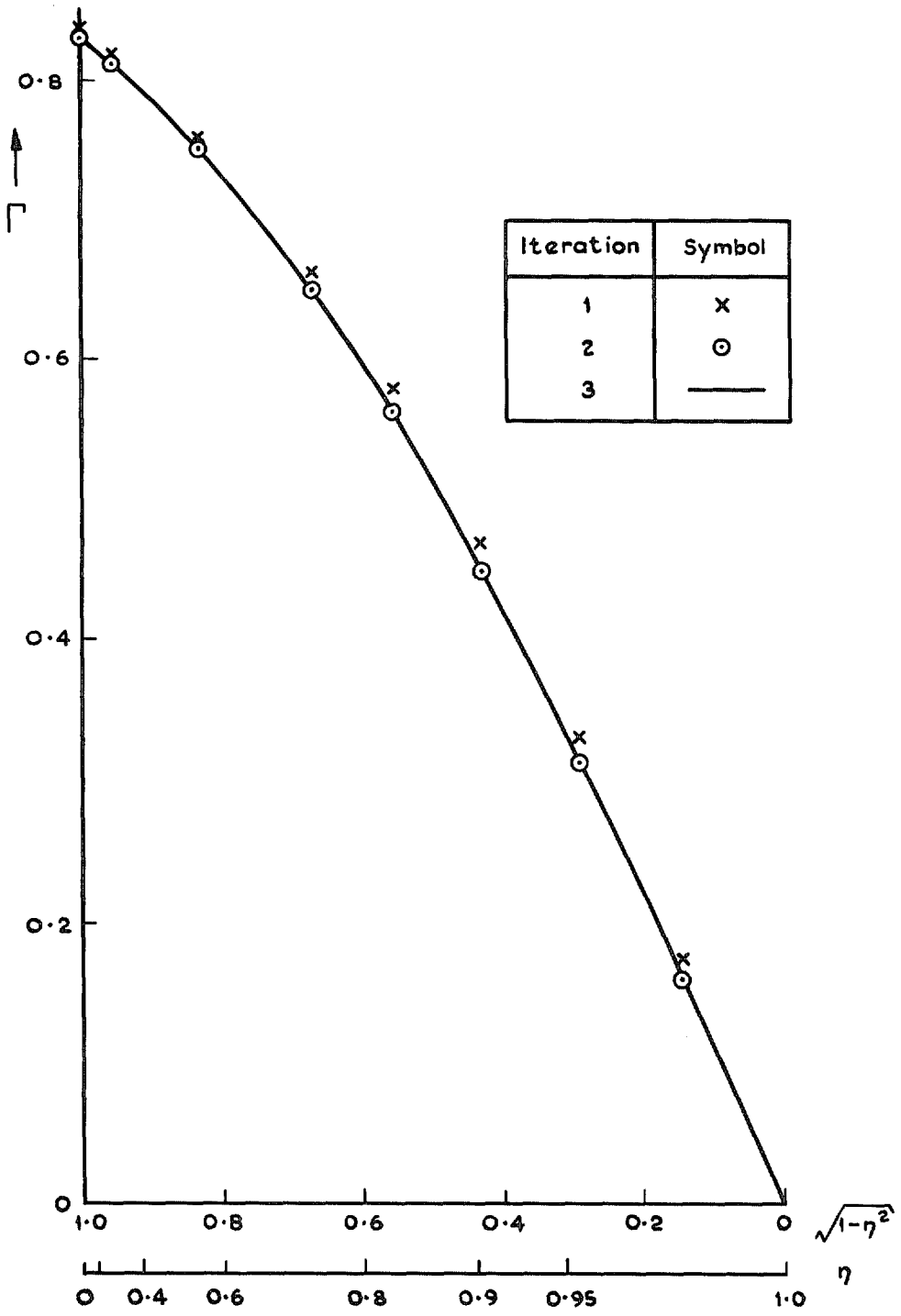

FIG. 3. Spanwise vorticity iterates for flat-plate rectangular wing, $A = 6$.

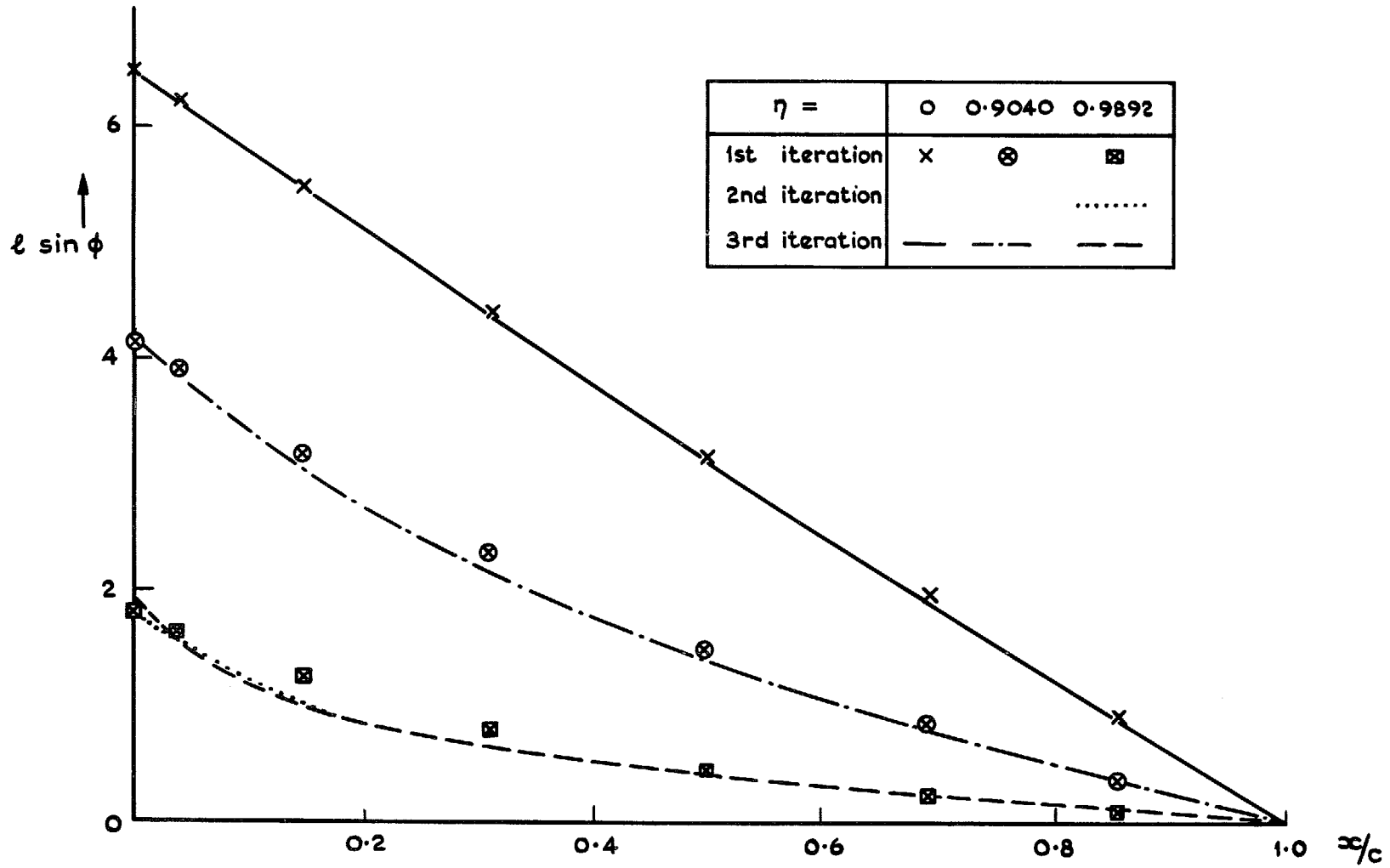

FIG. 4. Chordwise loading iterates for flat-plate rectangular wing, $A = 6$.

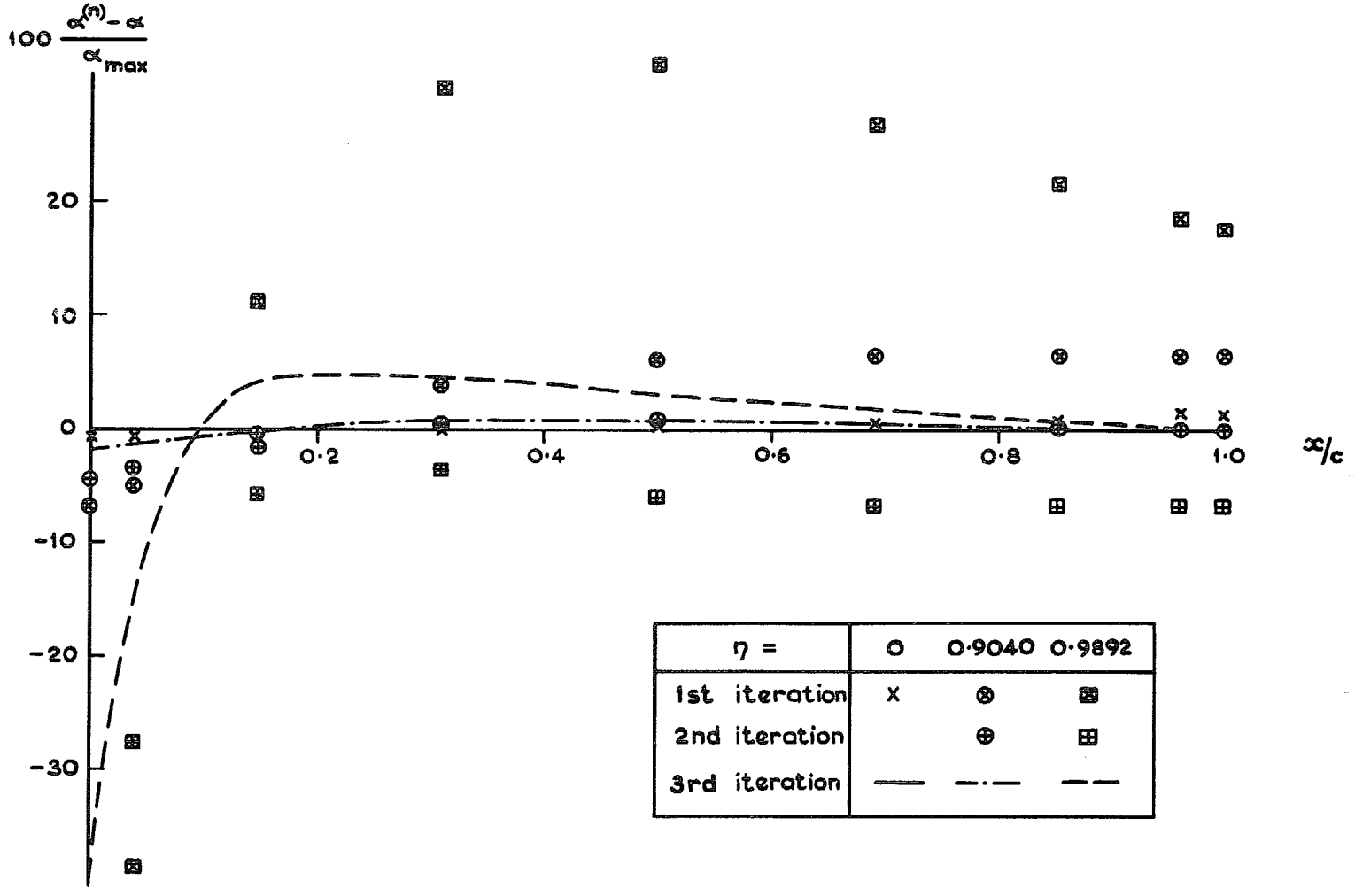

FIG. 5. Percentage downwash error iterates for flat-plate rectangular wing, $A = 6$.

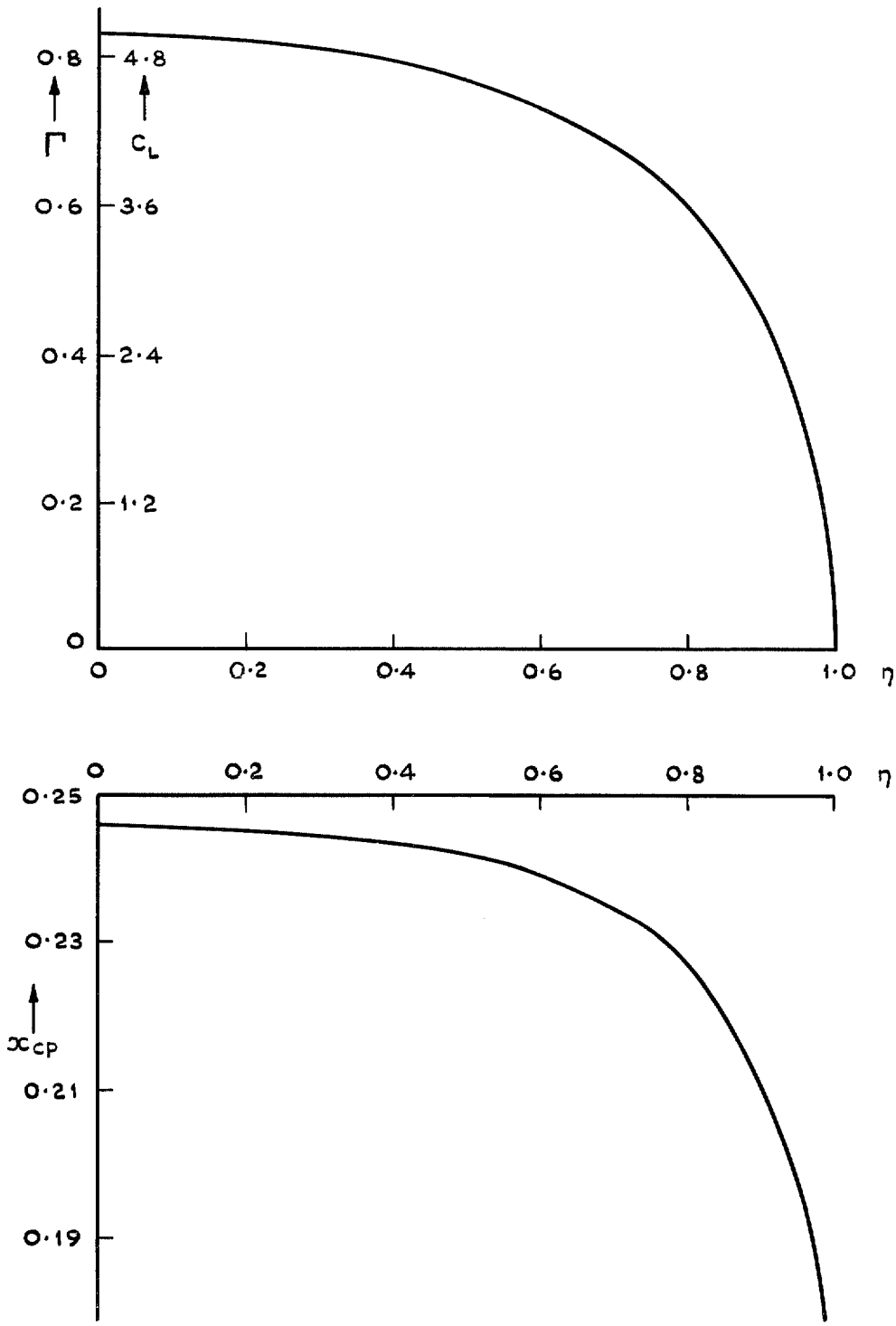

FIG. 6. Spanwise vorticity and centre of pressure for flat-plate rectangular wing, $A = 6$.

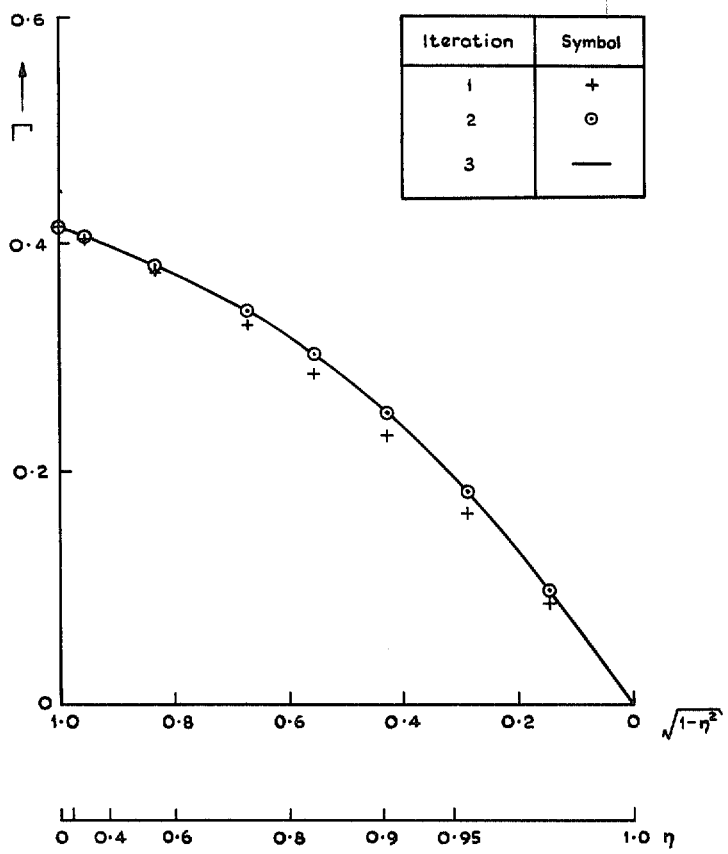

FIG. 7. Spanwise vorticity iterates for parabolic camber rectangular wing, $A = 6$.

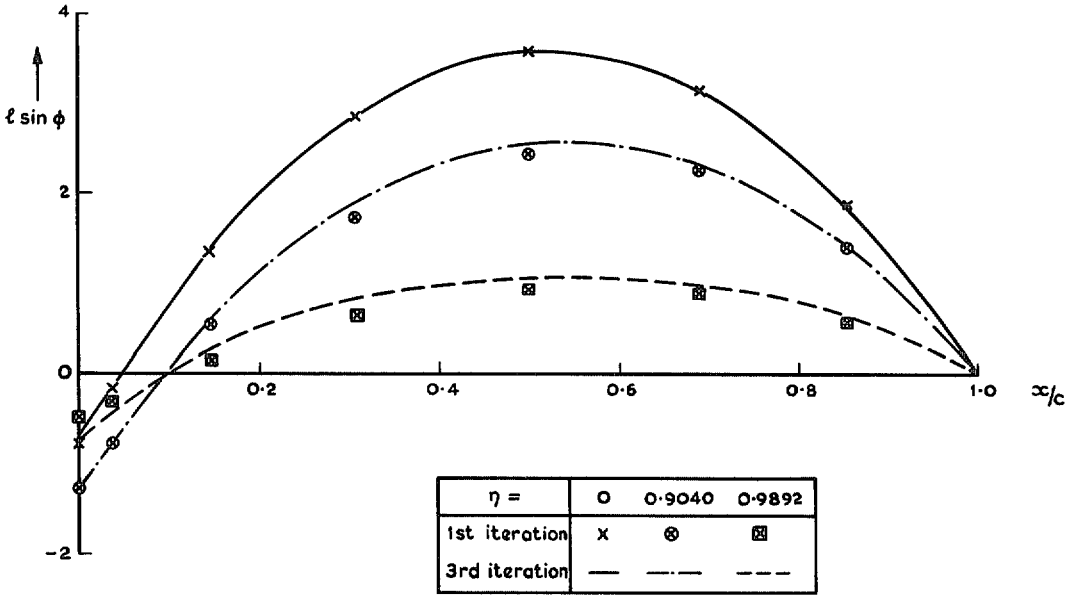

FIG. 8. Chordwise loading iterates for parabolic camber rectangular wing, $A = 6$.

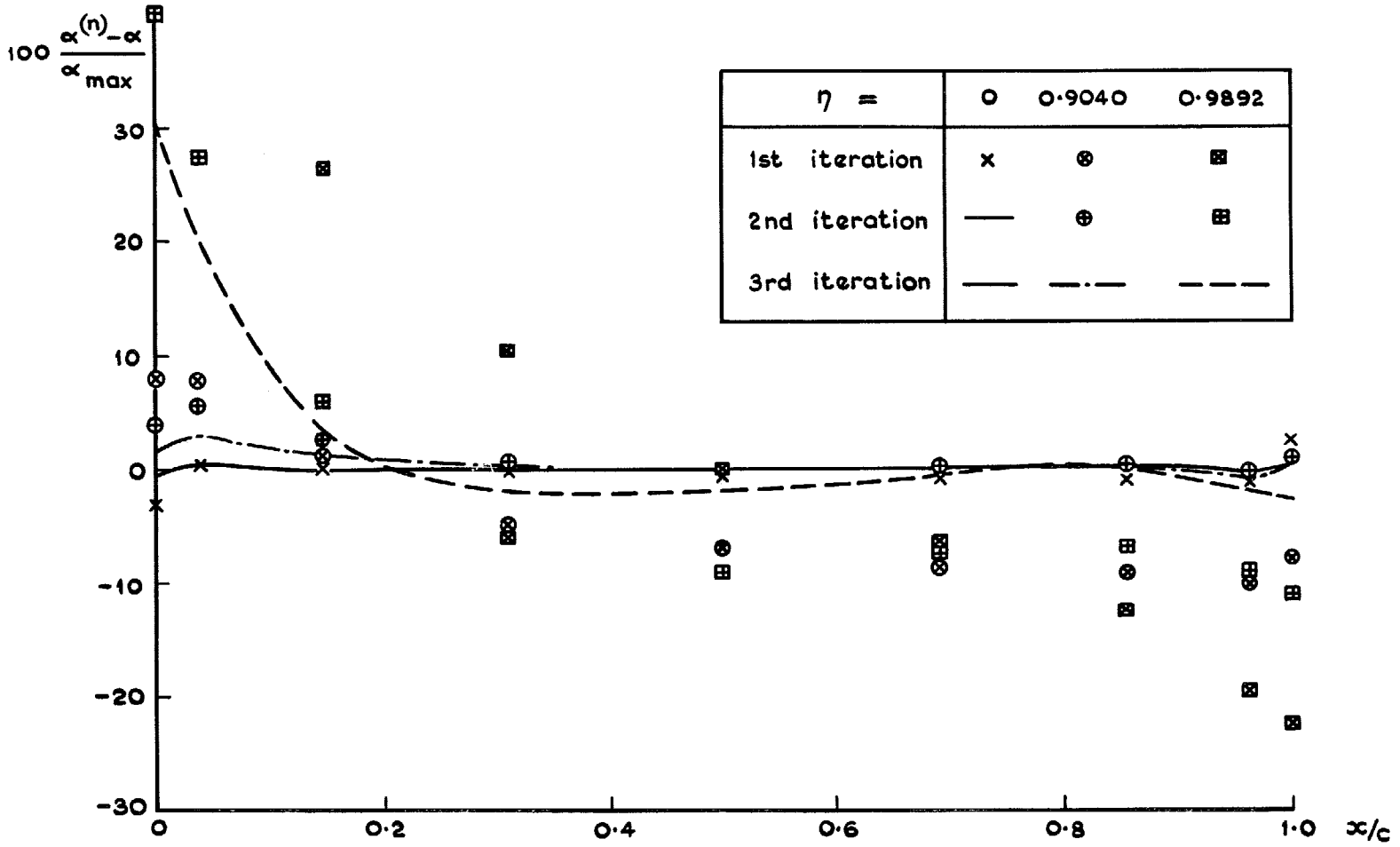

FIG. 9. Percentage downwash error iterates for parabolic camber rectangular wing, $A = 6$.

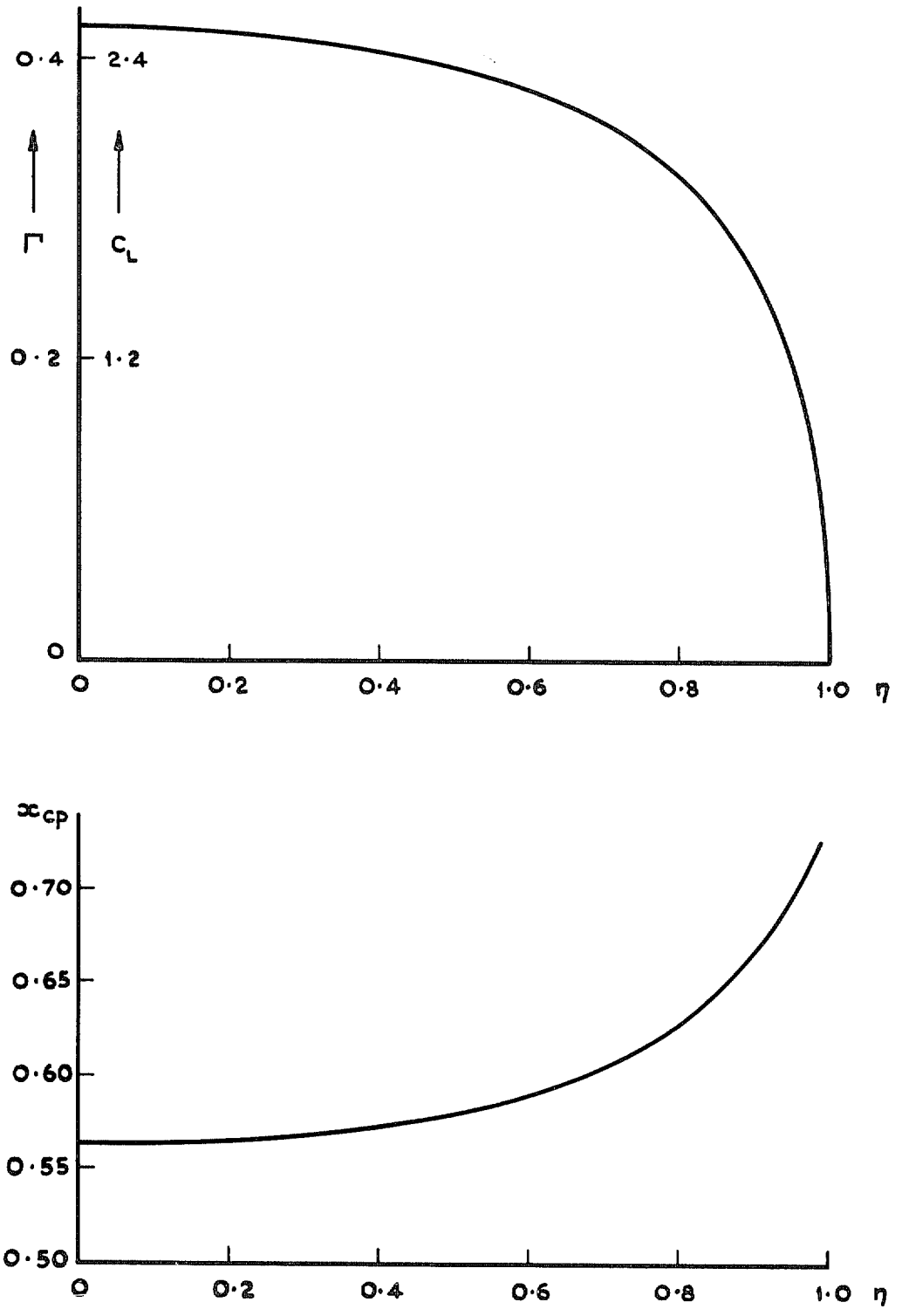

FIG. 10. Spanwise vorticity and centre of pressure for parabolic camber rectangular wing, $A = 6$.

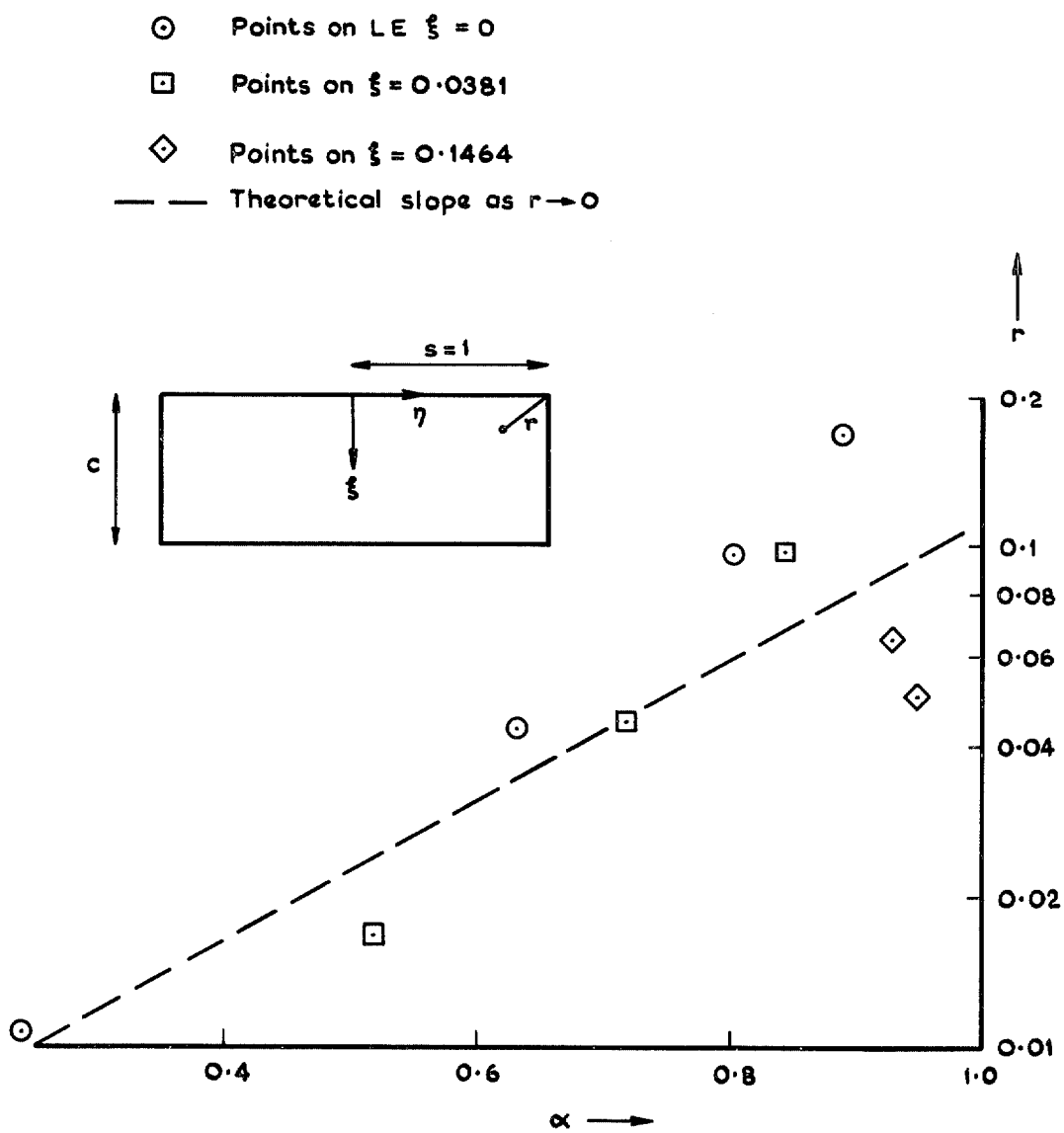

FIG. 11. Downwash field from Prandtl solution near LE tip.

Printed in England for Her Majesty's Stationery Office by J. W. Arrowsmith Ltd., Bristol BS3 2NT
Dd. 503426 K5 3/73

HER MAJESTY'S STATIONERY OFFICE

Government Bookshops

49 High Holborn, London WC1V 6HB
13a Castle Street, Edinburgh EH2 3AR
109 St Mary Street, Cardiff CF1 1JW
Brazennose Street, Manchester M60 8AS
50 Fairfax Street, Bristol BS1 3DE
258 Broad Street, Birmingham B1 2HE
80 Chichester Street, Belfast BT1 4JY

Government publications are also available through booksellers

R. & M. No. 371
SBN 11 470519